Net Recovery of UAV with Single-Frequency RTK GPS

Robert Skulstad Christoffer Lie Syversen Mariann Merz Nadezda Sokolova Thor I. Fossen Tor A. Johansen

Center for Autonomous Marine Operations and Systems (AMOS), Department of Engineering Cybernetics, Norwegian University of Science and Technology, Trondheim, Norway.

***Abstract*—A system for autonomous precision recovery of fixed-wing unmanned aerial vehicles (UAVs) using low-cost GPS L1 C/A based RTK (Real-Time Kinematic) solution utilizing locally generated corrections is described and field tested. We present a system architecture which includes the setup of the hardware and software for the onboard GPS receiver, base-station, differential link, computers running open-source carrier-phase positioning software, roll-stabilized GPS-antenna, dedicated flight control algorithms for the final approach, and their integration with the ArduPilot open-source autopilot in the small X8 UAV (flying-wing). Experimental results show proof-of-concept field tests where the prototype implementation has been used for recovery in a stationary recovery net.**

TABLE OF CONTENTS

1. INTRODUCTION

The launch and recovery phases pose significant challenges to the operation of UAVs, in particular for fixed-wing UAVs operating from smaller ships or other geographically or operationally constrained sites without a proper runway. While UAV missions can often be operated autonomously under pilot supervision via telemetry, the launch and recovery phases often require piloting using manual remote control (RC) and the pilot's visual feedback. Availability of reliable automatic recovery functionality with predictable performance is an important step towards increased autonomy that could potentially lead to reduced operating costs (no need for a skilled RC pilot) and improved safety records, and thereby enable increased use of UAVs.

It is widely accepted that in particular the vertical positioning based on a legacy GPS L1 C/A signal without any augmentation or differential corrections generally is not of sufficient accuracy for precision landing or recovery. High-precision automatic landing systems and methods for manned and unmanned aircraft have been based on GNSS augmented with differential data from one or more local base-stations (e.g [1], [2], [3], [4], [5], [6]), laser altimeters, radar altimeters [7], machine vision ([8], [9], [10]), or other radio navigation or augmentation systems. While optical systems such as laser and machine vision systems are highly limited by visibility and optical disturbances such as background and reflections, GNSS performance is primarily limited by radio frequency interference (RFI), multipath, ionospheric errors, as well as signal attenuation and blockage. For our intended applications, e.g. [11], [12], that may demand ship-based net recovery, the GNSS approach is expected to be favorable under a wider set of operational conditions that its alternatives, a conclusion also arrived at in [1], [3], [13], [14], [15]. Industry standards for GNSS ground-based augmentation systems (GBAS) and satellite-based augmentation systems (SBAS) are developed, [16], [17], [18], [1]. One one hand, high complexity and cost may render these systems infeasible for many of the operational scenarios involving small, low-cost UAVs, where higher risk and lower reliability may be acceptable. At the same time, while the DGNSS technique can provide single meter level positioning in optimal conditions, recovery in a net may in some cases require more stringent accuracy. To achieve this, the RTK technique is selected for this research. Due the short signal wavelength (19 cm for the GPS L1), the differential carrier phase processing can deliver centimeter level real time positioning when integer carrier phase ambiguities are successfully resolved, [19].

Some existing navigation methods used for GNSS-based automatic recovery and landing, e.g. [1], benefit heavily from dual-frequency differential or RTK positioning approaches. While multi-frequency GNSS receivers are generally high performance, they are also quite expensive. The present paper's main objective is to investigate autonomous recovery for small UAVs through the use of low-cost, single-frequency (L1) GPS receiver technology. This is enabled by open-source carrier-phase GNSS software - RTKLIB [20], [21] - that has recently become available for use. This software has been adopted for implementation of an RTK solution for use in the open-source autopilot software (ArduPilot) with custom functionality. While a dual-frequency carrier-phase GNSS would have the advantage of increased reliability and robustness (lower probability of degrading performance from a valid fix to a float solution due to more information to solve the integer ambiguity), faster acquisition of a valid fix solution, and potentially higher performance in terms of reduced latency and position error, the use of a single-frequency carrier-phase differential GNSS might still achieve centimeter level accuracy both horizontally and vertically, but with less reliability. Nevertheless, reliability and fault tolerance can be improved using various methods, including the use of inertial sensors [22], [23], [24], [1].

In this paper we describe a system architecture for autonomous recovery using single-frequency RTK technique. This includes a section containing an overview of the guidance, navigation and control (GNC) strategy chosen for the autonomous approach, followed by a section providing a more detailed description of the components that make up the approach and recovery system. In particular, this includes the setup of the hardware and software for the UAV's GPS receiver, base-station, the differential link, the computers running the open-source RTKLIB, the roll-stabilized GPS-antenna, the dedicated path planning, the guidance and flight control algorithms for the final approach, and their integration

Corresponding author: tor.arne.johansen@itk.ntnu.no
978-1-4799-5380-6/15/$31.00

with the open-source autopilot ArduPilot in the X8 flying-wing UAV. We then present experimental results from tests where the prototype implementation has been field tested for recovery in a stationary net, under fairly steady wind conditions.

2. AUTONOMOUS NET RECOVERY

The purpose of this section is to give an overview of the GNC tasks of the proposed recovery system. In particular, section 2 describes the generation of the desired path the UAV should follow towards the Landing Target (LT) where the recovery net is centered, while section 2 briefly discusses the principle of the single-frequency differential GNSS using RTK.

Flight paths

A waypoint (WP) marked LAND is placed at a convenient location relative to the Landing Target (LT). The LAND WP position might depend on several factors, such as winds, the distance and orientation of the landing net, the dynamic capabilities of the UAV, and the presence of terrain, buildings, other air traffic, and other obstructions and operational considerations. It is therefore considered outside the scope of this paper to discuss this issue in any further depth. When the UAV reaches the LAND WP, it switches to custom guidance controllers executing the Final Approach (FA) to recover the UAV. The first step is the calculation of the path, as well as an airspeed reference profile. The path altitude profile is illustrated in Figure 1 and the horizontal plane projection of the path is illustrated in Figure 2. Along the FA are some checkpoints (CPs): CP0 is identical to the LAND WP. CP2 is the final checkpoint defining a straight line towards the LT along the defined landing course. CP1 is the interception of a straight line from CP0 towards a circle that leads to CP2. Altitude is kept constant until CP1, where the glide slope is defined by a constant angle towards the LT, typically about 3 degrees as in conventional instrument landing systems (ILS).

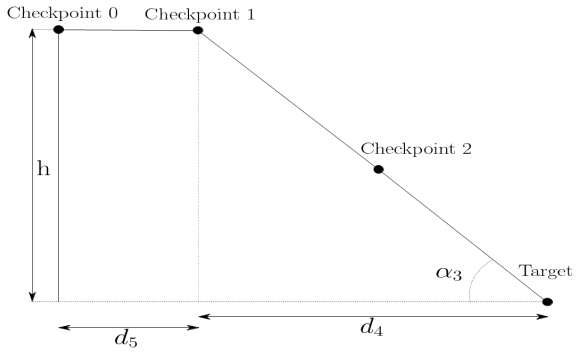

Figure 1. The reference altitude profile of the final approach.

For a LT with a fixed position and orientation a fixed base-line can be applied, while a moving landing-target requires a moving base-line. The field tests reported in this paper uses a moving base-line RTK. Hence, the landing course and CPs can be continuously adjusted, and the measurement processing is set up for moving baseline navigation that can achieve precision relative positioning but less accurate absolute positioning.

Airspeed could be kept constant, decreased or increased towards the LT, depending on the stability of the aircraft in

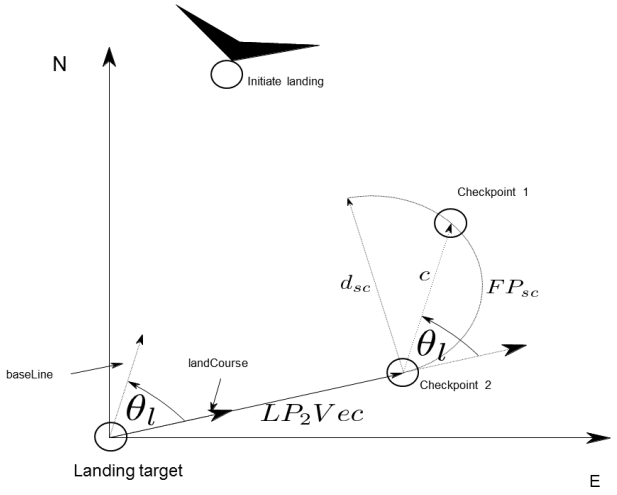

Figure 2. The reference horizontal path of the final approach.

the prevailing winds and landing course. It is outside the scope of the present paper to provide a general algorithm for generating the airspeed profile since it may depend on the UAV capabilities, as well as operating conditions. Generally speaking, low airspeed will minimize impact and risk of structural damage when hitting the LT, while sufficiently high airspeed is necessary in order to ensure stability and adequate control authority for precise control during FA.

After CP2 is passed, the flight control system monitors the airspeed, altitude and cross-track errors. In addition the status of the navigation system used for recovery is monitored for performance degradation detection. If the UAV is not able to follow the references with sufficient accuracy, and landing is allowed to be aborted by the automatic control system, the FA will be aborted with an evasive maneuver in order to go around and hold or start over with another landing attempt. When the UAV is sufficiently close to the LT, the engine is stopped in order to minimize the risk of damage to the system. We refer to [25] for further details on these issues.

As will be shown in later sections, precision recovery depends on accurate control of altitude, cross-track error and airspeed. The feedback loops should be based on accurate and low-latency measurements in order to allow tight tuning of the flight controller's gains.

Real-Time Kinematic

Recovery in a net or other small-area landing target typically requires position tracking accuracy of less than 1 meter. This leads to stricter requirements for navigation and control than the ones necessary for many other UAV operations. We investigate the use of single-frequency carrier-phase GPS based on Real-Time Kinematics (RTK) augmented by differential corrections. Carrier phase based techniques achieves orders of magnitude more accurate positioning compared to stand-alone GNSS, and also allow much higher accuracy than what is possible using differential code measurement processing, [19]. Unfortunately, the carrier-phase approach requires more advanced signal processing and is generally more sensitive to noise and other adverse effects such as multipath signal reflections. While code-based GPS processing has a well-defined unique solution for the position, the carrier-phase GPS has an ambiguity corresponding to an integer number

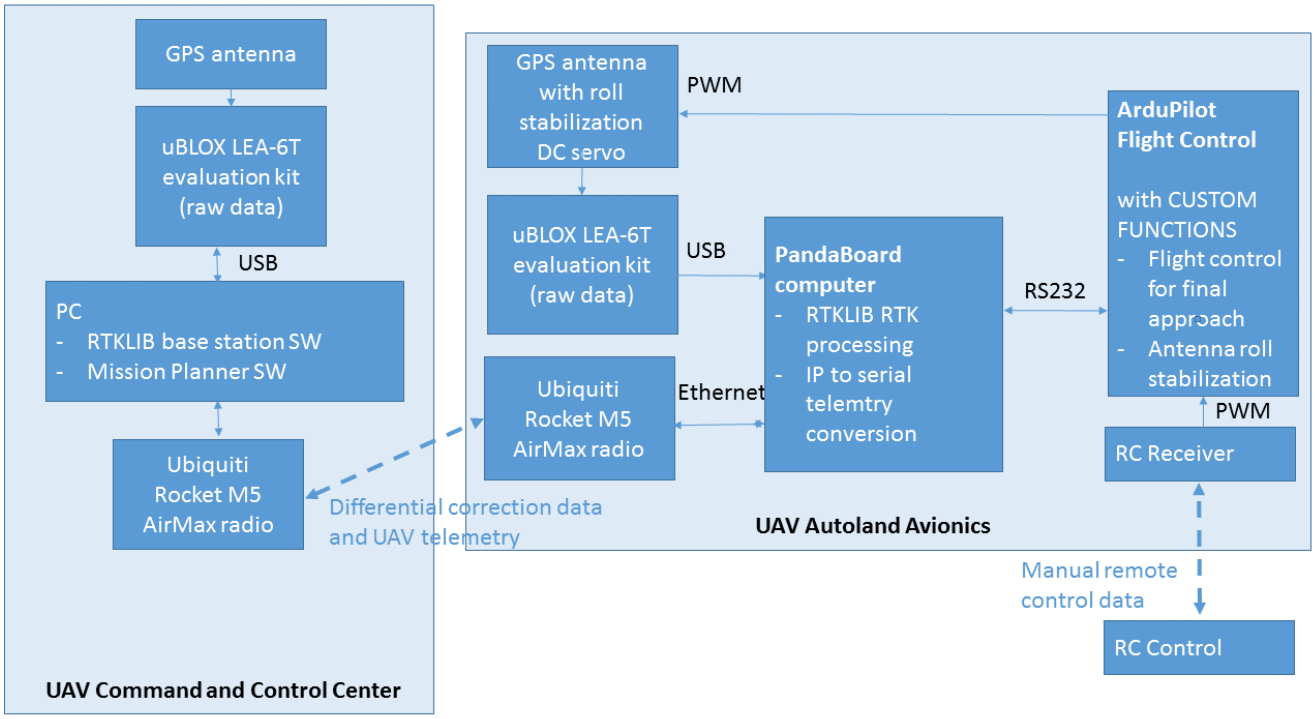

Figure 3. Main avionics components in UAV and ground Command and Control Center used during field testing.

of carrier wavelengths (19 cm) that must be resolved, [19]. When the ambiguity is resolved with a sufficiently high degree of certainty, this is referred to as a FIX solution, while otherwise the solution degrades to a FLOAT solution where the ambiguity is allowed to be a decimal or a floating point number, leading to a decimeter level accuracy. When the float solution cannot be achieved, the DGPS or in the worst case the stand-alone GPS approach is applied, commonly referred to as a SINGLE solution.

A local GNSS base-station provides the data needed for differential processing over a wireless communication link from the base-station to the UAV. This system allows the pseudo-ranges and carrier phases from a set of common satellites to be corrected for certain common-mode errors influencing the transmission of the GNSS signals from the satellites in space to the ground, assuming the base station is so close to the UAV that the received GNSS signals from a sufficient number of common satellites are degraded in the same way. With a base-station installed within no more than some kilometers from the landing target, one can make effective corrections for most of the errors under normal ionospheric conditions, e.g. [1], [6], [7], [15]. It should be mentioned that criteria for deciding if a FIX solution is valid (i.e. the integer ambiguity resolution is correct) is a complex issue that is currently subject to research.

3. System Description

The recovery system described above can be implemented in various ways using hardware and software components. In the field tests presented in this paper, we used a combination of low-cost hardware, open-source software, and custom software. The intended test bed was an X8 flying wing from Skywalker Technology Co. powered by a 800 W electric motor. This was believed to provide a capable and inexpensive platform, although with certain limitations regarding payload weight and size and also with respect to maneuverability and control aspects. The components described below were selected with these limitations in mind. Figure 3 illustrates the main components used, and additional details are provided in the following sections.

Single-frequency carrier-phase RTK

The u-Blox-LEA-6T GPS receiver is used in both the UAV and base-station since its firmware provides raw carrier phase and pseudo-range measurements along with the computed position and velocity solution. For convenience in the prototype implementation used for the field experiments, an evaluation kit with USB connection was chosen. A Tallysman TW2105 embedded precision L1 GPS patch antenna was mounted on an aluminum ground plane on a roll-stabilization assembly inside the fuselage of the X8 UAV. The EPO (expanded polyolefin) material used for the X8 fuselage does not attenuate the transmission of the L1-frequency signal in any significant way.

The RTK computations on-board the UAV were executed on a Pandaboard single-board computer having a dual-core ARM processor with clock frequency of 1.2 GHz. The open source RTKLIB [21] was run under Linux to produce the RTK solution with the following key settings after careful evaluation and testing of the alternatives, [25]: 5 Hz update rate, "Airborne < 4g", "fix-and-hold" integer ambiguity resolution, receiver dynamics off, elevation mask on 15 degrees, minimum 5 valid satellites required, RAIM FDE off, PRN exclusion off, and use of default ionospheric and tropospheric models, [21]. Data was transmitted from the Pandaboard to the ArduPilot using the NMEA serial data protocol, with a custom expansion to include the 3-dimensional baseline

vector along with quality indicators of the RTK solution. As a result, the ArduPilot reads a total of 3 standard NMEA messages in addition to the custom message on a RS232 serial line, [25].

The differential correction data from the base-station was transmitted as UDP packets to the Pandaboard over a wireless AirMAX (similar to WiMAX) TDMA data-link using Ubiquiti Rocket M5 2x2 MIMO broadband radios at 5.8 GHz. Since raw carrier phase measurements are transmitted, a data rate of about 12 kbit/sec are typically required for the RXM-RAW and RXM-SFRB messages only. In addition, the telemetry data between the ArduPilot and Mission Planner share the same digital data link. These radio communication modules allow considerable robustness, operational flexibility and range with networked operation as multiple access points, relay stations and multiple antenna configuration.

Precise Point Positioning (PPP) static mode was used to calibrate the position of the base station and static recovery net.

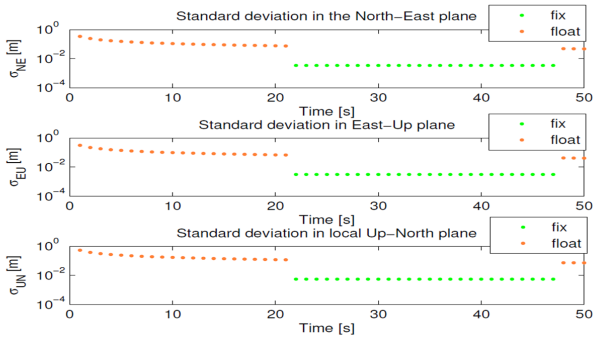

Figure 4. The standard deviation of the postioning error achieved.

Figure 4 shows the standard deviation of the positioning error reported by the RTKLIB software with FLOAT and FIX solutions, in an ideal static condition. We observe that standard deviation better than 1 cm in all axes is achieved with a FIX solution, while the standard deviation of the FLOAT solution is on a decimeter level. We note that due to possible undetected errors in the integer ambiguity resolution, a bias may be present and dominate the total error. Moreover, in a dynamic condition experienced during flight the accuracy is expected to be further degraded, in particular due to the processing and serial communication latency in the GPS receiver and Pandaboard computer that may exceed 200 ms.

Roll-stabilization of antenna

With the GPS antenna and its ground plane mounted at a fixed location and attitude in the UAV, the signals received by the GPS receiver are influenced by the attitude of the UAV. In particular, while the ground plane is intended to attenuate multi-path reflections, it will at high roll and pitch angles also attenuate the signals from low elevation satellites that are located in the shadow of the ground plane. For example, the tests in Figure 5 shows that the number of received satellite signals sometimes drops from 8 to 6 or 7 with roll angles of about 30 degrees or more. This degrades the positioning performance as the solution may degrade from FIX to FLOAT not only while the roll angles are high but also during a recovery period until a FIX solution is achieved again. This may in particular occur between CP1 and CP2

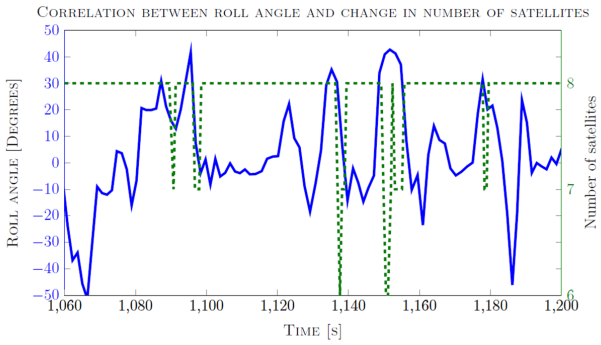

Figure 5. The number of satellites available together with the UAV roll angle (no roll compensation of the the GPS antenna).

during the banked turn before the last straight leg of the final approach leading to degraded or unacceptable performance. It might also occur during the straight leg of the FA due to disturbances caused by strong turbulence and unsteady winds.

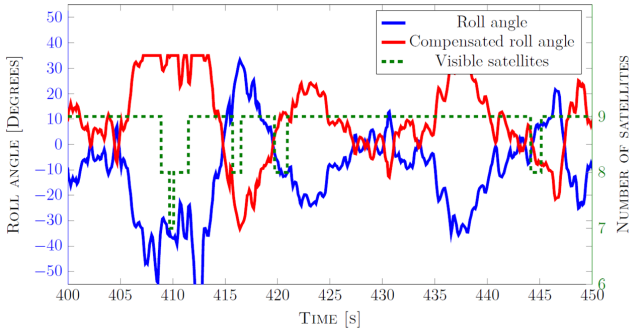

Figure 6. The number of satellites available together with UAV roll angle (with up to 35 degrees roll compensation of GPS antenna).

In order to improve the performance of the RTK and reduce the risk of degrading the solution from FIX to FLOAT during high roll angles, the GPS antenna may be placed on a simple roll-compensation assembly driven by a DC servo. Since the roll angle of the UAV is measured by the auto-pilot using an Inertial Motion Unit (IMU), the DC servo position can be directly commanded to compensate for the UAV roll angle. In our field tests, the effect of this compensation is illustrated in Figure 6. Due to space restrictions near the roll-compensated GPS antenna inside the fuselage, its compensation is limited to about 35 degrees. The results indicate that the roll compensation seems to have a positive effect and that the number of satellites visible to the GPS receiver is less reduced by the roll motion. While a similar compensation of pitch angle motions might also have benefits, it was not implemented because it was considered less important and due to the additional complexity with weight and space required of a two-axis mechanism for compensation of both roll and pitch. Yaw compensation is not needed due to the symmetry of the antenna.

Flight control algorithms

A block diagram illustrating the custom flight control loops used during the FA is given in Figure 7. The lateral

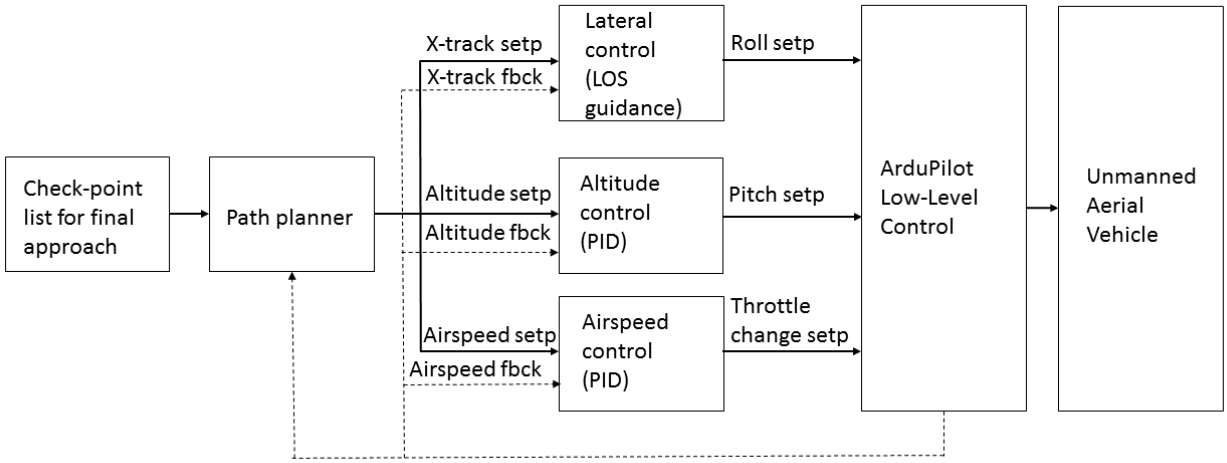

Figure 7. Block diagram illustrating the main flight control loops used during final approach for automatic precision landing.

(cross-track error) control is ArduPilot's existing Line-of-Sight (LOS) guidance law, [26], extended with coordinate transformation needed to convert positions to a East-North-Up coordinate frame relative to the moving baseline, see [25] for details. The longitudinal (airspeed and altitude) control loops are different from the existing ArduPilot control laws, and implemented as decoupled PID controllers, in order to achieve better control accuracy. In addition, landing target data was transmitted from the Mission Planner to the Ardupilot as a custom telemetry function.

This functionality is implemented by modifying the open-source firmware of the Ardupilot. In addition, some extensions to the visualization in the Mission Planner was included to provide the UAV pilot with information on the CPs and LT in order to verify correct functionality and behaviour of the UAV.

Figure 8. NTNU's X8 flying-wing UAV used for flight tests.

4. Results

Test setup

The system was installed in a relatively small (approximately 2.1 meter wing span) X8 flying-wing UAV, cf. Figure 8, and a recovery net was installed at the Breivika test field in Agdenes where the main tests were conducted, see Figure 9. All tests were conducted as Visual Line of Sight (VLOS) operations under Remotely Piloted Aircraft System (RPAS) rules, with shortest possible distance and duration of the final approach.

The X8 is launched by catapult, has a nominal airspeed at about 17 m/s, and an endurance of about 1 hour in our configuration. It is tailless and has only two control surfaces, one elevon on each wing. Turn rate is thus controlled by the bank angle.

Flights tests

The reported flight tests were conducted on 1st June 2014. In the morning and early afternoon, all tests were conducted in calm air (negligible winds), while the final testing in the late afternoon and early evening experienced light, smooth headwinds. It should be noted that the speed-controller used measured ground speed (from the GPS) rather than measured airspeed in these tests due to a hardware issue. With the low wind speeds during the tests, the difference is expected to be small.

Table 1 shows some statistics of the RTK solution during the flight tests. The statistics are collected during the total test time, not only final approach, and contains extensive periods with manual RC flying where the pilot makes sharp turns and dives where RTK FIX is lost. Further analysis of the data are given in [25]. Approximately 20 approaches were flown on this day, most of these were terminated with a fly-through of a LT where the net was replaced by two horizontal crepe ribbons that assists visual observation of deviation from LT. Only the two last approaches were flown toward the actual net (resulting in impact and the risk of structural damage).

Figure 10 shows the performance from two FAs with the autonomous net recovery system active. The setpoint for ground speed was 15 m/s which is somewhat low and the control authority is not sufficiently high for the cross-track controller to make the error sufficiently low in the first flown case, thus leading to a failure of the recovery since the error is

Figure 9. The recovery net used, approximate 5 x 3 meters.

Table 1. RTK/DGPS solution during testing 1st June 2014.

Start time (UTC)	Fix (%)	Float (%)	Single (%)	Satellites	Duration (min)
07:14	25.9	74.1	0	10-12	48
08:36	35.3	64.7	0	8-11	44
10:14	32.7	67.3	0	7-9	40
11:53	44.7	54.5	0.8	6-8	45
13:31	49.6	48.5	1.9	7-9	43
14:50	25.2	74.8	0	7	18
16:27	29.7	70.3	0	9-10	40
18:10	60.0	39.1	0.9	5-7	4

3 meters when the LT is reached. This shows the importance of relatively high speed during the final approach in order to achieve sufficiently accurate control of the X8. At the recovery point, only the right wing of the X8 impacted the net, causing the UAV to spin around and come to rest a couple of meters behind the landing net. However, the X8 escaped the event without structural damage proving the robustness of this platform. The second attempt successfully demonstrated net recovery as the X8 impacted the net less than 1 meter from the center point in both the vertical and horizontal direction. Figure 12 shows the path and RTK GPS status during the second flown case.

Figure 13 shows the performance from five representative final approaches with the system active. In these tests, the setpoint for ground speed was 17 m/s and the last leg of the FA is significantly shorter than in the above mentioned tests, compare Figures 11-12 with Figures 14-18. It is observed that in all cases the cross-track and altitude errors are relatively small such that the net recovery can be considered successful with the given size of the net and X8 UAV. We remark that the cross-track controller is not aggressive in order to avoid oscillations. In addition, with the speed-controller not being optimally tuned, a sudden increase in throttle to correct for speed errors could lead to severe changes in cross-track if the lateral controller was aggressively using the roll angle to quickly reduce the cross-track error. Hence, in order to decouple the lateral and longitudinal dynamics, a slow control towards desired path was used.

It should be noted that during some of the final approaches reported in Figures 10 and 13 we do not have a FIX but rather a FLOAT solution with some positive validation ratio value (eq. (E.7.18) in [21]) being below threshold of 3.0 selected for FIX, but still non-zero. It provides a baseline vector with standard deviation equal to that of the float values seen in Figure 4, i.e. about decimeter level standard deviation. The

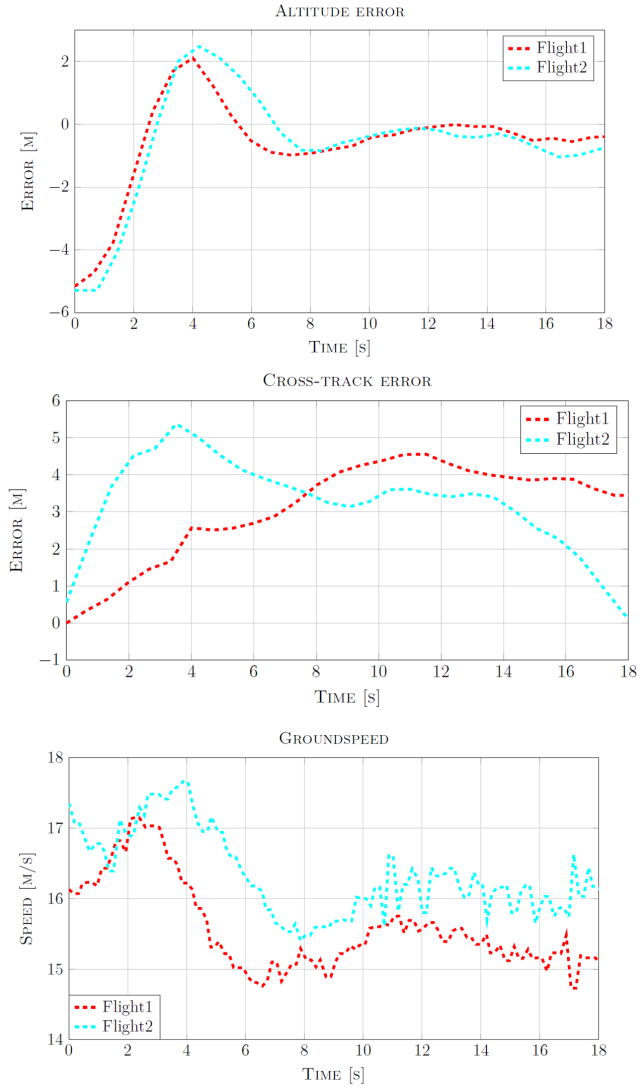

Figure 10. Field tests with two final approaches on the same day.

tests indicate that with a sufficient positive validation ratio, FLOAT solution quality may provide acceptable performance during FA. Examples of this are given in Figures 11-12 and Figures 14-18.

Discussion

The results provides a proof of concept for the low-cost/single-frequency RTK-based UAV precision recovery. The tested prototype has many weaknesses and potentials for improvements that should be pursued in order to develop a system that has consistently high accuracy and reliability. Among the most important aspects are the following:

- Improved tuning of the flight controllers, and optimization of operating conditions such as airspeed reference and location of checkpoints depending on wind conditions. These appear to be the main limitations of performance observed during the tests.
- Improvements in the UAV's GNSS antenna, placement, ground plane and cabling in order to provide the best possible receiver conditions.

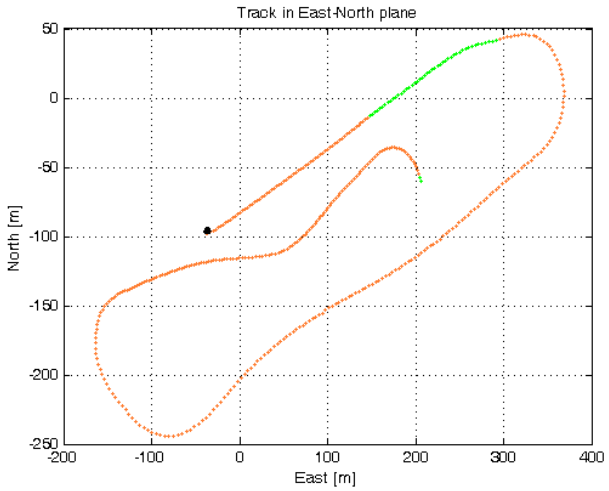

Figure 11. Flight path and RTK GPS status during final approach towards South-West (test 1 of 2). Green indicates FIX, orange indicates FLOAT, and red indicated SINGLE solution. The origin is at the GPS base station, and the LT is the black mark.

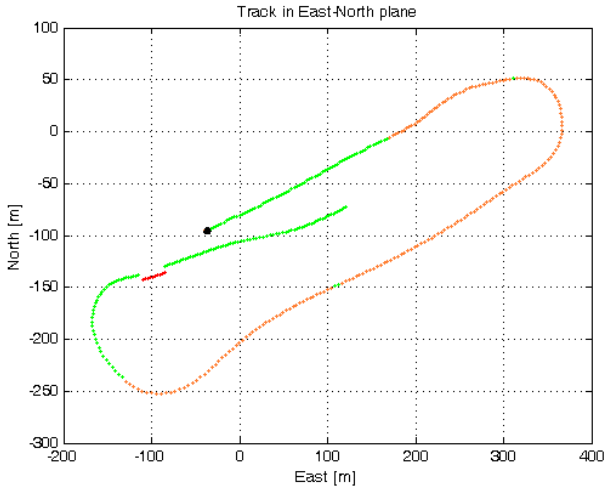

Figure 12. Flight path and RTK GPS status during final approach towards South-West (test 2 of 2). Green indicates FIX, orange indicates FLOAT, and red indicated SINGLE solution. The origin is at the GPS base station, and the LT is the black mark.

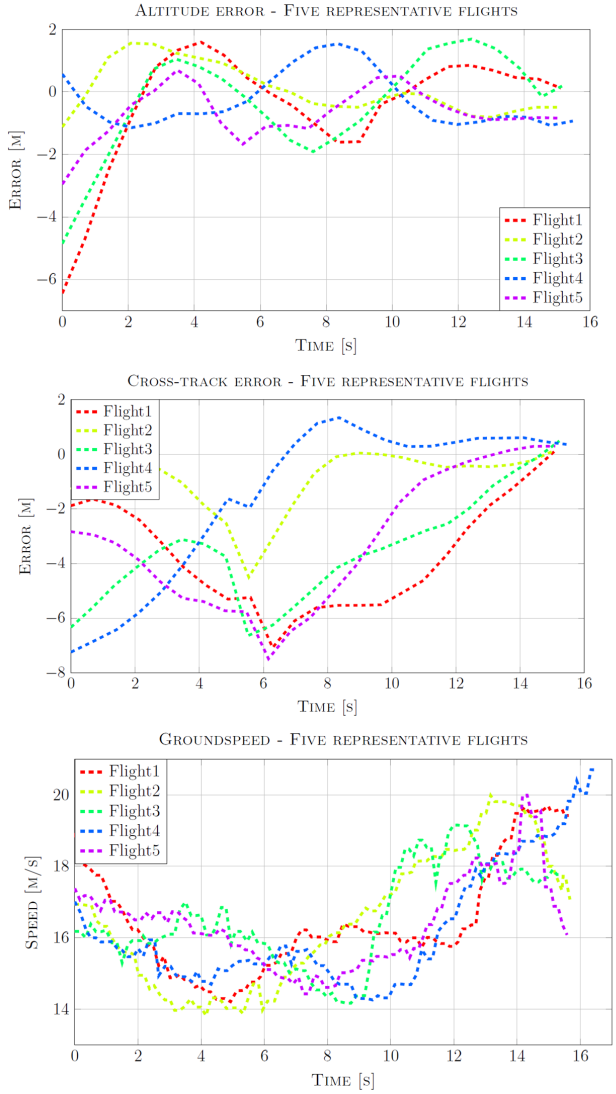

Figure 13. Field tests with five final approaches on the same day.

- Use of a low-cost GNSS receiver that could exploit GLONASS and GALILEO satellites is expected to improve the reliability and validity of RTK FIX.
- Use an IMU or other redundant position sensors for fault tolerance in cases when GPS navigation degrades, has outages, or the carrier-phase ambiguity resolution is not valid. Although our research has the focus on civilian applications where jamming and spoofing are not considered to be threats, other adverse conditions such as unintentional interference or poor satellite geometry are still relevant. While the RTK accuracy is normally sufficient for precision recovery, the reliability and integrity of the system are of more concern.
- Use of an IMU for compensation for GNSS receiver and RTK computational latency, allowing higher bandwidth of the control loops. With valid RTK fix the navigation and control accuracy is more limited by latency than other positioning error.
- Refine and test functionality for autonomous evasive maneuvers and initiate new recovery attempts upon detection of navigation system faults or other conditions that may lead to recovery failure, see [25] for preliminary results. A primary concern is autonomous procedures for handling faults or abnormal conditions that occurs late during the FA, close to the point when evasive maneuvers may not be safe. Relevant methods may be IMU-based dead reckoning.
- Hardware implementation with lower weight and size, and better system integration.
- A more suitable user interface allowing the pilot to better monitor and evaluate the performance and status of the autonomous recovery system, hence allow the pilot to better judge when it is necessary to override the system.
- Further test of moving baseline and checkpoint updating approaches on moving landing targets such as recovery nets on small ships.

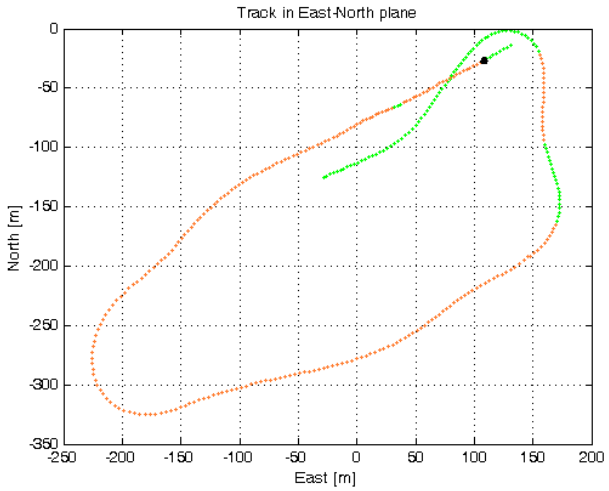

Figure 14. Flight path and RTK GPS status during final approach towards North-East (test 1 of 5). Green indicates FIX, orange indicates FLOAT, and red indicated SINGLE solution. The origin is at the GPS base station, and the LT is the black mark.

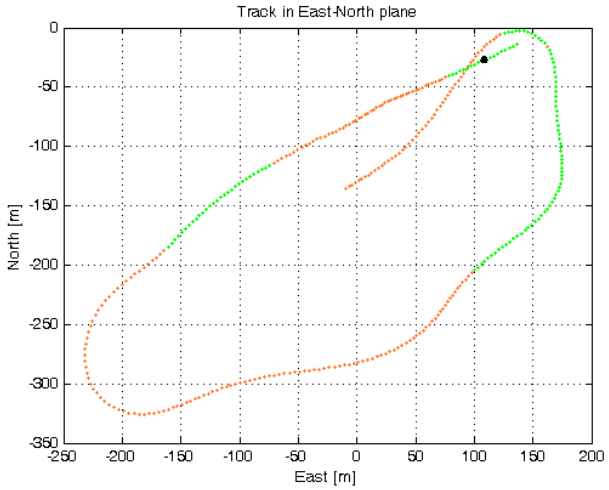

Figure 15. Flight path and RTK GPS status during final approach towards North-East (test 2 of 5). Green indicates FIX, orange indicates FLOAT, and red indicated SINGLE solution. The origin is at the GPS base station, and the LT is the black mark.

5. Conclusions

A relatively simple system for autonomous net recovery of small fixed-wing UAVs has been designed and field tested. The system is based on low-cost hardware such as single-frequency GPS receivers, broadband radio communication, and open source software for flight control and RTK computations. The flight tests with a prototype implementation demonstrate successful UAV recovery with the UAV hitting the center of the landing net with less than 1 meter error horizontally and vertically. This provides a proof-of-concept, although the tests also show the need for certain improvements in order to achieve the desired accuracy and reliability of the flight control and GNSS solution.

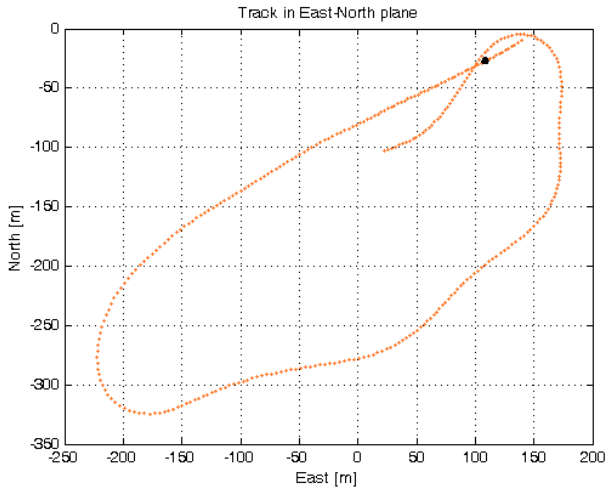

Figure 16. Flight path and RTK GPS status during final approach towards North-East (test 3 of 5). Green indicates FIX, orange indicates FLOAT, and red indicated SINGLE solution. The origin is at the GPS base station, and the LT is the black mark.

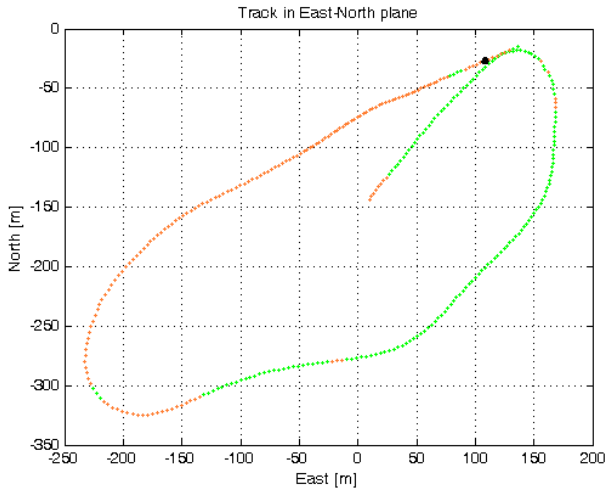

Figure 17. Flight path and RTK GPS status during final approach towards North-East (test 4 of 5). Green indicates FIX, orange indicates FLOAT, and red indicated SINGLE solution. The origin is at the GPS base station, and the LT is the black mark.

Acknowledgments

This work was supported by the Research Council of Norway through the Centers of Excellence funding scheme, Project number 223254 - Centre for Autonomous Marine Operations and Systems (AMOS), as well as Innovation Norway through the project Unmanned Maritime Aerial Surveillance Systems with Maritime Robotics AS. The authors are grateful for the assistance provided by the engineers at NTNU and Maritime Robotics AS, in particular Lars Semb, Carl Erik Stephansen and Torkel Hansen.

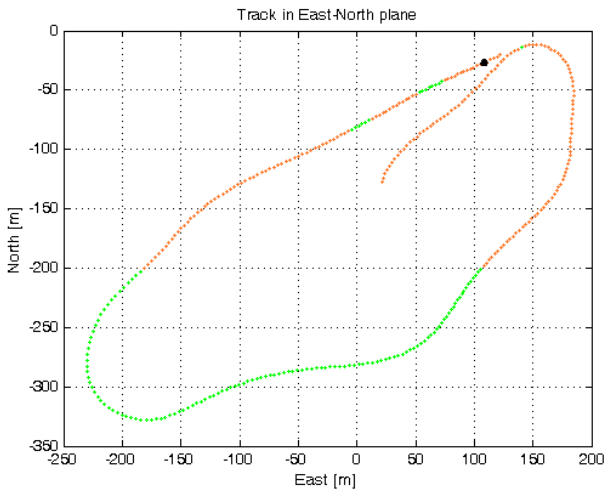

Figure 18. Flight path and RTK GPS status during final approach towards North-East (test 5 of 5). Green indicates FIX, orange indicates FLOAT, and red indicated SINGLE solution. The origin is at the GPS base station, and the LT is the black mark.

REFERENCES

[1] J. Rife, S. Khanafseh, S. Pullen, D. D. Lorenzo, U.-S. Kim, M. Koenig, T.-Y. Chiou, B. Kempny, and B. Pervan, "Navigation, interference suppression, and fault monitoring in the sea-based joint precision approach and landing system," *Proc. IEEE*, vol. 96, pp. 1958–1975, 2008.

[2] R. M. Kalafus and P. Braisted, "System for using differential GPS receiver with autopilot systems for category III precision approaches," Patent US 6 342 853B1, 2002.

[3] B. Pervan, F.-C. Chan, D. Gebre-Egziabher, S. Pullen, P. Enge, and G. Colby, "Performance analysis of carrier-phase DGPS navigation for shipboard landing of aircraft," *J. Navigation*, vol. 50, pp. 181–191, 2003.

[4] S. Pullen, P. Enge, and J. Lee, "Local-area differential GNSS architecture optimized to support unmanned aerial vehicles (UAVs)," in *Proceedings of ION ITM, San Diego, CA*, 2013.

[5] A. Cho, J. Kim, S. Lee, S. Choi, B. Lee, B. Kim, N. Park, D. Kim, and C. Kee, "Fully autonomous taxiing, takeoff and landing of a UAV using a single-antenna GPS receiver only," in *Proc. Int. Conf. Control, Autmation and Systems, Seoul, Korea*, 2007.

[6] T. Murphy, J. Ackland, T. Imrich, T. Lapp, and R. Freidman, "Early operational experience with new capabilities enabled by GBAS landing systems (GLS)," in *Proceedings of the 2006 National Technical Meeting of The Institute of Navigation, Monterey, CA*, 2006, pp. 468–478.

[7] T. Murphy, "Global navigation satellite system landing systems and methods," Patent US 7 373 223 B2, 2008.

[8] S. Huh and D. H. Shim, "A vision-based automatic landing method for fixed-wing UAVs," *J. Intelligent and Robotic Systems*, vol. 57, pp. 217–231, 2010.

[9] H. J. Kim, M. Kim, H. Lim, C. Park, S. Yoon, D. Lee, H. Choi, G. Oh, J. Park, and Y. Kim, "Fully autonomous vision-based net-recovery landing system for a fixed-wing UAV," *IEEE/ASME Transactions on Mechatronics*, vol. 18, pp. 1320–1333, 2013.

[10] O. Yakimenko, I. I. Kaminer, W. J. Lentz, and P. A. Ghyzel, "Unmanned aircraft navigation for shipboard landing using infrared vision," *IEEE Transactions on Aerospace and Electronic Systems*, vol. 38, no. 4, pp. 1181–1200, Oct 2002.

[11] V. E. Hovstein, A. Sægrov, and T. A. Johansen, "Experiences with coastal and maritime UAS BLOS operation with phased-array antenna digital payload data link," in *Int. Conf. Unmanned Aerial Systems (ICUAS), Orlando*, 2014.

[12] M. Faria, J. Pinto, F. Py, J. Fortuna, H. Dias, R. Martins, F. Leira, T. A. Johansen, J. Sousa, and K. Rajan, "Coordinating UAVs and AUVs for oceanographic field experiments: Challenges and lessons learned experiments in UAV and AUV control for coastal oceanography," in *Proc. IEEE Int. Conf. Robotics and Automation, Hong Kong*, 2014.

[13] D.-J. Huang and S.-S. Jan, "Availability analysis of RTK for UAV shipboard landing," in *Proceedings of the 2014 International Technical Meeting of The Institute of Navigation, San Diego, California*, 2014, pp. 629–637.

[14] I. I. Kaminer, O. A. Yakimenko, V. N. Dobrokodov, M. I. Lizarraga, and A. M. Pascoal, "Cooperative control of small UAVs for naval applications," vol. 1, 2004, pp. 626 – 631.

[15] M.-B. Heo and B. Pervan, "Carrier phase navigation architecture for shipboard relative GPS," *IEEE Trans. Aerospace and Electronic Systems*, vol. 42, pp. 670–679, 2006.

[16] "Minimum operational performance specification for global navigation satellite ground based augmentation system ground equipment to support category i operations," Tech. Rep. ED-114A, EUROCAE, March 2013.

[17] "Minimum operational performance standards for GPS local area augmentation system airborne equipment," Tech. Rep. RTCA SC-159, WG-4, DO-253C, Washington, DC, 2008.

[18] "Minimum operational performance standards for global positioning system/wide area augmentation system airborne equipment," Tech. Rep. RTCA SC-159, WG-2, DO-229D, Washington, DC, 2006.

[19] M. S. Grewal, L. R. Weill, and A. P. Andrews, *Global Positioning Systems, Inertial Navigation, and Integration*. Wiley-Interscience, 2007.

[20] T. Takasu and A. Yasuda, "Development of the low-cost RTK-GPS receiver with an open source program package RTKLIB," in *Proc. International Symposium on GPS/GNSS*, 2009.

[21] T. Takasu, "Rtklib ver. 2.4.2 manual. http://www.rtklib.com/prog/manual_2.4.2.pdf," Tech. Rep., April 2013.

[22] G. Loegering and S. Harris, "Landing dispersion results - Global Hawk autoland-system," in *AIAA's 1st Technical Conference and Workshop on Unmanned Aerispace Vehicles*, 2002.

[23] M. D. McIntyre and L. R. Anderson, "Inertially augmented GPS landing system," EP 1 014 104A2, 2006.

[24] L. R. Anderson, S. B. Krogh, M. D. McIntyre, and T. Murphy, "Skipping filter for inertially augmented landing system," Patent US 6 549 829 B1, 2003.

[25] R. Skulstad and C. L. Syversen, "Low-cost instrumentation system for recovery of fixed-wing UAV in a net," 2014, master thesis, Department of Engineering Cybernetics, Norwegian University of Science and Technology, Trondheim.

[26] S. Park, J. Deyst, and J. P. How, "A new nonlinear guidance logic for trajectory tracking," in *In Proceedings of the AIAA Guidance, Navigation and Control Conference*, 2004.

BIOGRAPHY

Robert Skulstad *received the Msc in Engineering Cybernetics in 2014 at the Norwegian University of Science and Technology and in 2012 the BEng in Automation Engineering at Aalesund University College. He wrote the Master's thesis, along with Christoffer Lie Syversen, from which this article is based.*

Christoffer Lie Syversen *Received the MSc degree in Engineering Cybernetics from Norwegian University of Science and Technology in 2014. Currently works as a project engineer in Kongsberg Defence and Aerospace. He wrote the Master's thesis, along with Robert Skulstad, from which this article is based.*

Mariann Merz *(née Jansen) received her BSc in Aerospace Engineering and Mechanics from the University of Minnesota, Minneapolis, Minnesota, USA in 1999, and her MSc in Aerospace Engineering from the same institution in 2001.She is currently working on a PhD related to Unmanned Aerial Vehicle technology at the Norwegian University of Science and Technology. Since February 2008 she has been a Research Scientist with the SINTEF Information and Communication Technology (ICT) group in Trondheim, Norway. While at SINTEF ICT she has been involved with projects ranging from Air Traffic Management Research (through participation in SESAR) to Safety and Reliability projects in the Oil and Gas Industry. Earlier work history, includes working as an Autoflight Systems Analyst with The Boeing Company from 2001 to 2007, working as a Teacher Assistant at the University of Minnesota from 1999 to 2000, and employment as a Co-op Engineer in the Performance Engineering group with Northwest Airlines from 1997 to 1999.*

Nadezda Sokolova *received her PhD degree in 2011 from Norwegian University of Science and Technology (NTNU), where she worked on weak GNSS signal tracking and use of GNSS for precise velocity and acceleration determination. She also holds a MSc degree in Geomatics Engineering from University of Calgary, Canada, and a MSc degree in Space and Aeronautical Engineering from Narvik University College, Norway. Currently, she is a research scientist at SINTEF ICT, Communication Systems department and adjunct associate professor at the Centre of Excellence on Autonomous Marine Operations and Systems (AMOS), NTNU. Her primary research interests are in the areas of Global Navigation Satellite Systems and their augmentation via inertial and other secondary data sources.*

Professor Thor I. Fossen *received the MSc degree in Naval Architecture and the PhD in Engineering Cybernetics in 1987 and 1991 both from the Norwegian University of Science and Technology. He was elected into the Norwegian Academy of Technological Sciences in 1998. Fossen has graduated more than 150 master students and he is the main supervisor of 27 PhD candidates. He is teaching, mathematical modelling of aircraft, marine craft, unmanned vehicles and nonlinear control theory. Fossen has authored approximately 300 scientific papers and 5 textbooks including the Wiley textbooks Guidance and Control of Ocean Vehicles and Handbook of Marine Craft Hydrodynamics and Motion Control. Fossen is one of the co-founders of Marine Cybernetics where he was Vice President R&D in the period 2002-2008. His paper on weather optimal positioning control of marine vessels received the Automatica Prize Paper Award in 2002. In 2008 he received the Arch T. Colwell Merit Award.*

Professor Tor Arne Johansen *(MSc and PhD from the Norwegian University of Science and Technology, Trondheim) worked at SINTEF as a researcher before he was appointed Associated Professor at the Norwegian University of Science and Technology in Trondheim in 1997 and Professor in 2001. He has published several hundred articles in the areas of control, estimation and optimization with applications in the marine, automotive, biomedical and process industries. In 2002 Johansen co-founded the company Marine Cybernetics AS where he was Vice President until 2008. Prof. Johansen received the 2006 Arch T. Colwell Merit Award of the SAE, and is currently a principal researcher within the Center of Excellence on Autonomous Marine Operations and Systems (AMOS) and director of the Unmanned Aerial Vehicle Laboratory at NTNU.*